A Computational Study to Understand the Surface Reactivity of Gold Nanoparticles with Amines and DNA

Boon-Kin PONG[1], Jim-Yang LEE[1,2], **Bernhardt L. TROUT**[1,3]

[1]Singapore-MIT Alliance, National University of Singapore, 4 Engineering Drive 3, Singapore 117583, Singapore

[2]Department of Chemical and Biomolecular Engineering, National University of Singapore, 10 Kent Ridge Crescent, Singapore 119260, Singapore

[3]Department of Chemical Engineering, Massachusetts Institute of Technology, 77 Massachusetts Avenue, Cambridge, Massachusetts 02139, USA

Abstract **We conducted a computational adsorption study of methylamine on various surface-models of gold nanoparticle which is facetted by multiple {111} and {100} planes. In addition to these flat surfaces, our models include the stepped surfaces (ridges) formed along the intersections of these planes. Binding on the flat surfaces was fairly weak, but substantially stronger on the ridges by an average of 4.4 kcal/mol. This finding supports the idea that ssDNA's interaction with gold nanoparticles occurs through the amines on the purine/pyrimidine rings. Also, this typically undesirable interaction between DNA and gold nanoparticles is expected to increase as the particle size decreases. Our analysis suggests that particle size is an important controlling parameter to reduce this interaction.**

Index Terms **— adsorption, density functional theory, DNA, gold nanoparticles, methylamine**

I. Introduction

Gold nano-spheres (AuNS) have become one of the most commonly studied metallic nanoparticles for the development of bioanalytics assays, particularly the detection of sequence specific DNA molecules. This is due in part to the relative ease of synthesizing stable AuNS of controlled size with narrow size distribution. Also, AuNS exhibit optical and electronic properties that can be exploited in a variety of detection methodologies [1,2]. Recently, AuNS have been demonstrated to quench the fluorescence of organic dyes [3] and CdSe/ZnS core-shell nanocrystals [4-9] (quantum dots) when they are brought to close proximity by DNA linkers. Reversible quenching of photoluminescence is central to the working principal of molecular beacons used to detect single stranded DNA (ssDNA). Quantum dots exhibit a number of superior qualities over the organic molecular dyes; they are generally brighter, photo-stable, have narrow emission bandwidths and can be excited by a single excitation UV source. These qualities make quantum-dot-based molecular beacon highly attractive. To be successfully used in molecular beacon assembly, quantum dots must be able to undergo reversible quenching by another moiety at close proximity. The use of gold nanoparticle as a quencher for quantum dots have been demonstrated in a number of studies [4-9].

Molecular beacons based on AuNS will entail DNA hybridization events in which one end of the single-stranded DNA (ssDNA) probes is tethered to AuNS. These ssDNA-AuNS bioconjugates are routinely prepared using modified ssDNA probes with an alklythiol group (-RSH) attached to the 3' or 5' end. For optimal efficiency, these surface-immobilized ssDNA probes should suspend freely in the solution. Evidence, however, suggests that interaction with the gold surface prevents these linear DNA molecules from extending freely into the solution. Pristine, non-thiol-modified DNA was found to bind strongly onto evaporated Au film and have reduced hybridization efficiency [10]. The stability of poly(dT)-stabilized AuNS increases with the length of the oligonucleotide, whereas the stabilities of poly(dA)- and poly(dC)-stabilized colloids were only slightly affected by the DNA chain length [11]. This sequence-dependent stability was attributed to *weaker* interaction of dT with the gold nanoparticle surface; weak side-chain interaction allows the particle surface to bond

We thank the Singapore-MIT Alliance program for financial support

with a greater number of poly(dT) molecules through the thiol-modified ends. Jang [12] studied the binding chemistry of the DNA nucleosides on 13nm gold nanoparticles and found the adsorption rates of dT much *slower* than those of dA, dC and dG. Taken together, DNA's affinity to AuNS surface is strongly affected by its nucleoside composition, of which dT contributes the least binding. Fig. 1 shows the chemical structures of the four deoxynucleosides. The key features that distinguish dT from the other three nucleosides are the absence of a primary amine and the presence of a methyl and second aromatic carbonyl. Because primary alkylamines have been observed to adsorb strongly onto gold nanoparticles [13,14], we propose that the primary amines on the three deoxynucleosides (dC, dA and dG) account for the interaction between DNA and gold surfaces.

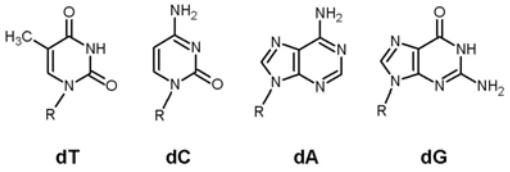

Fig. 1. Chemical structures of the four deoxynucleosides in DNA, where -R is a deoxyribose sugar. Only dT lacks a primary amine.

Interaction between amines and gold surface has mostly been regarded to be very weak and hence of little significance. For example, octadecylamine form ordered monolayers gold thin films using vapor phase deposition only under well-controlled conditions [15]. However, this self-assembly failed when the gold surface was immersed in high polarity solution such as ethanol, a phenomenon the authors attributed to competitive interaction of solvent molecules with the amine. A radically different situation emerged, however, when the gold surfaces are that of a nano-sized particle. Water solubilized citrate-stabilized AuNS (diameter ~3.5 nm) were quickly and quantitatively transferred into toluene by treating the hydrosol with octadecylamine [13]. Clearly, the reactivity of nano-particulate gold towards amines is much higher than that of bulk gold. Given the probable relevance that this interaction has to hybridization on AuNS-DNA bioconjugates, there is a need to understand better the nature of this strong interaction. Kumar et. al. investigated the nature of binding between alkylamines and AuNS (diameter ~5 nm) and found two modes of binding on the gold nanoparticles, corresponding to TGA (thermogravimetry analysis) weight losses at ~260^{o}C and ~510^{o}C [14]. Also, characterization of these amine-functionalized gold nano-crystals showed that the amine-gold interaction can be described by a weak covalent bond [16]. To the best of our knowledge, there have been no theoretical studies on the nature of the interactions between amines and AuNS. The closest theoretical knowledge can be drawn from an adsorption study of cystein, HS-CH_2-$CH(NH_2)$-COOH, on bulk gold [17]. It was found that in addition to binding at the thiol end, the amine group can also form a N-Au bond at the surface (bond strength ~6 kcal/mol). However, we note that in this case the amine-gold interaction was conformationally constrained since the cystein was bound more tightly at the thiol end. Using first principle computational methods, our work aims to provide an understanding of the origin of strong binding between amines and nano-particulate gold surfaces. Based on this understanding, we develop hypotheses on the interactions between ssDNA and gold nanoparticles. Although the more complex ssDNA molecule will interact with the gold surface in a more complicated manner, our analysis provides a plausible explanation of experimental observations.

II. Theoretical Calculations

High-resolution transmission electron microscopy imaging of 2.4 nm AuNS showed that they adopt a truncated octahedral TO geometry with well defined {111} and {100} facets [18]. This concurs with predictions by molecular dynamics simulations [19]. Fig. 2 shows the TO structure of a nano-size particle. We studied methylamine binding on four different types of surfaces present on these gold nanoparticles. The four surfaces are the flat (111) and (100) surfaces, and the *ridges* along which these planes intersect. Our calculations were performed in the framework of density functional theory (DFT) with the gradient-corrected PW91 exchange-correlation functional. The GNU publicly licensed software DACAPO [20] was used to perform the calculations. For all computations, the electronic wavefunctions were expanded from a basis set of planewaves with kinetic energy cutoff of 25 Ry, and the surface Brillouin zones were sampled at 4×4×1 Monkhorst-Pack k-points. All the periodic slab-geometry unit cells have a vacuum layer of about 13Å, so that the adsorbate is always isolated from the upper slab by about 10Å. Methylamine (CH_3NH_2), the simplest alkyl amine, was used in this study to investigate the binding of primary amines on nanoparticulate gold surfaces.

Our slab models for the Au(111) and Au(100) surfaces consist of three atomic layers with a repeat vacuum height of about 13Å above it, with 9 gold atoms constituting each unit-cell layer. We also studied the two types of ridges, which are formed between the intersecting {111}/{111} planes and {111}/{100} planes. Our approach to model these ridge surfaces was to remove selectively a few adjacent surface atoms from a Au(111) slab, effectively forming the stepped surface found on the TO particle. Fig. 2 shows the unit-cell slabs used in our study. Note the two stepped surfaces are unique, which are formed by

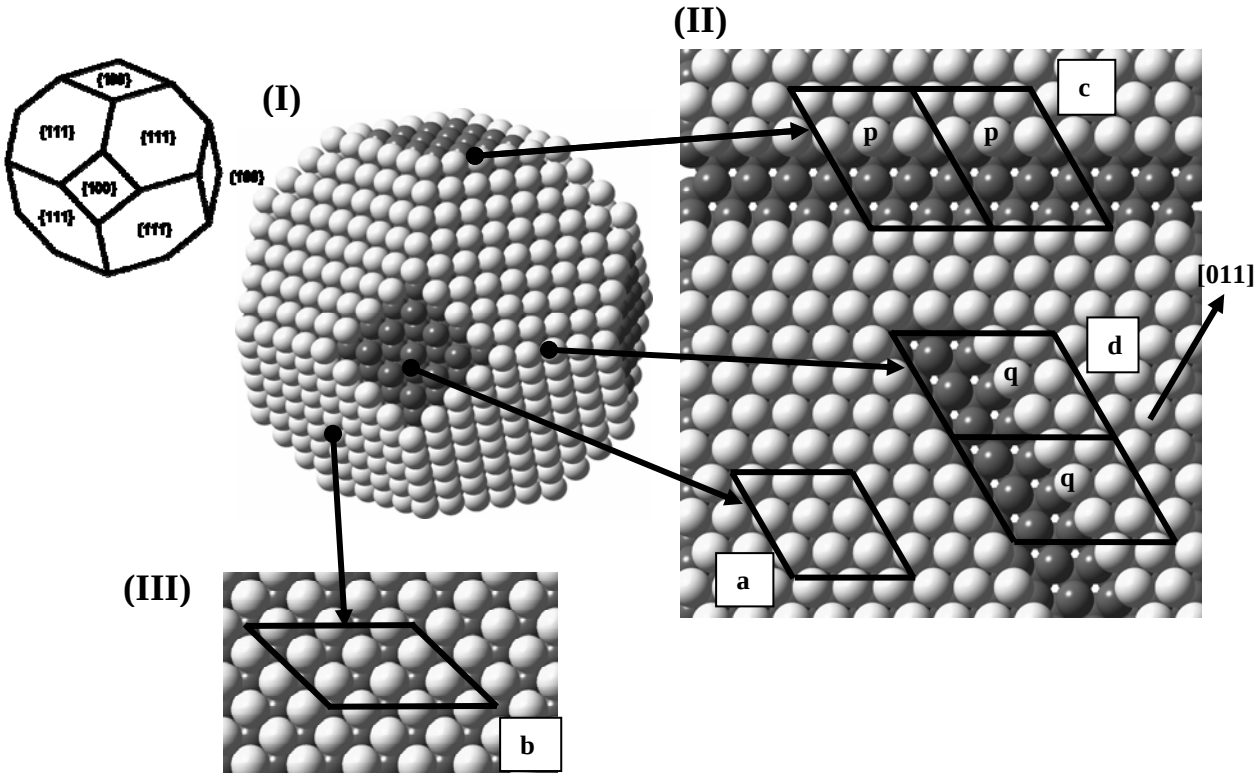

Fig 2. Four different types of surface on nanospherical gold were investigated in this study. **(I)** Truncated octahedral structure of a spherical gold nanoparicle, with inset indicating the {111} and {100} planes. **(II)** Plan view of Au(111) surface with three atomic layers (bottom layers darkened for clarity). Unit cell **a** models the flat (111) surface, unit cell **d** models the stepped surface between {111}/{111} ridge; unit cell **c** models the stepped surface between {111}/{100} ridge. For the stepped surfaces, methylamine adsorption was examined around **p** and **q** atoms. **(III)** Plan view of Au(100) surface with unit cell **b** to model the flat (100) surface.

removing rows of Au atoms traversing different directions. Also, larger unit cells containing 12 atoms per layer were used for the ridge surface models to ensure that the periodic slabs produce "valleys" of sufficient width. Note that the atomic arrangements of Au atoms at our stepped surfaces are precisely that of the real ridges on the nanocrystal.

The binding activity of methylamine on the gold surfaces was investigated at various sites on the slabs. All our unit cell slabs were three atomic layers thick; an additional fourth Au layer was found to affect the binding energy by less than 0.3 kcal/mol. All of the atoms, except those of the bottom-most Au layer, were allowed to relax and optimization was terminated when the residual force was smaller than 0.05eV/Å. The binding energy (BE) of the amine is then computed as: $BE = E_{Au} + E_{MA} - E_{Au\text{-}MA}$, where E_{Au}, E_{MA} and $E_{Au\text{-}MA}$ are the total energies of the clean gold surface, free methylamine and adsorbate-gold, respectively. We first determined the lattice constant of face-centered cubic gold to be 4.18Å (experimental 4.08Å [21]). The slightly higher lattice constant determined here is typical for DFT calculations employing the PW91-GGA exchange-correlation functional [22]. The computationally determined lattice constant of 4.18 Å was used for all calculations to minimize inter-atomic strains.

I. Results & Discussions

On the flat surfaces, methyl amine was found to adsorb exclusively with a single gold atom at the *atop* site via its nitrogen atom; no binding was found on all the other high-symmetry sites. That the amine interacts with only one Au atom may be rationalized by the small size of nitrogen and its maximum coordination number at four. Binding energies at the atop site of the (111) and the (100) surfaces are 10.8 and 12.7 kcal/mol respectively. Similar to its adsorption on the flat surfaces, methylamine binds to the stepped surfaces through interaction with a single Au atom located on the ridge. Importantly, the binding energies on the stepped surfaces are significantly higher at 16.6 and 15.7 kcal/mol on the {111}/{111} and {111}/{100} ridge surfaces respectively. Table 1 and Fig. 3 summarize the binding energy and geometries on the four surfaces.

Table 1. Binding energy, bond distance and geometry of methylamine adsorption on four different surface types on gold nanoparticles. (See text for binding energy corrected for aqueous phase.)

	Surface Type			
	Au(111)	**Au(100)**	**Ridge {111}/{111}**	**Ridge {111}/{100}**
Binding Energy, gas phase (kcal/mol)	10.8 (10.9)[a]	12.7	16.6 (16.8)[a]	15.7
Binding Energy, aqueous (kcal/mol)	3.4	5.3	9.2	8.3
N-Au bond distance (Å)	2.38	2.34	2.27	2.30
Au-N-C angle (^{o})	118.4	118.5	120.2	119.7

a – data in parentheses are binding energies when an additional Au layer was added to the unit cells.

At this point, we have shown that methylamine binds significantly stronger on the ridged surfaces of Au nanocrystals than on the flat surfaces by an average of 4.4 kcal/mol. This represents a preferential binding on the ridge surface over the flat surface by a factor over 900 (estimated from the relation $\Delta G=-RT\ln K_{eq}$, and neglecting entropic effects at room temperature). Note that our calculations were performed for gas phase interactions. In water, the energetics of amines is likely to be affected by hydrogen-bond formation with water molecules. An approximate correction may be applied to our results by considering the effects of adsorption on amine's H-bonding with water molecules. In water, amines form H-bonds through hydrogen and their nitrogen lone electron pair. In the adsorbed state, the nitrogen lone pair site is bonded to an Au atom and hence becomes inaccessible to water molecules, while the hydrogens remain free to interact with water molecules. The energy penalty for sorption in water may hence be approximated by the loss of H-bond at the nitrogen, which has been calculated to be 7.4 kcal/mol [23]. Our DFT computations also showed that methylamine (as a H-acceptor) binds to a water molecule (as a H-donor) with a binding energy of 6.9 kcal/mol. When we apply this approximate energy penalty to our results, the binding energies on the flat surfaces are reduced to 3.4 and 5.3 kcal/mol on Au(111) and Au(100), respectively. Entropic loss on the surface-bound state may further reduce binding strengths. Via this perspective, amine binds only moderately to flat gold surfaces in an aqueous environment. Binding on AuNS remains fairly strong on the ridges at 9.2 ({111}/{111}) and 8.3 ({111}/{100}) kcal/mol. Based on this analysis, we conclude that the peculiar reactivity of AuNS towards amines occur from the ridge surfaces on these multi-facetted particles.

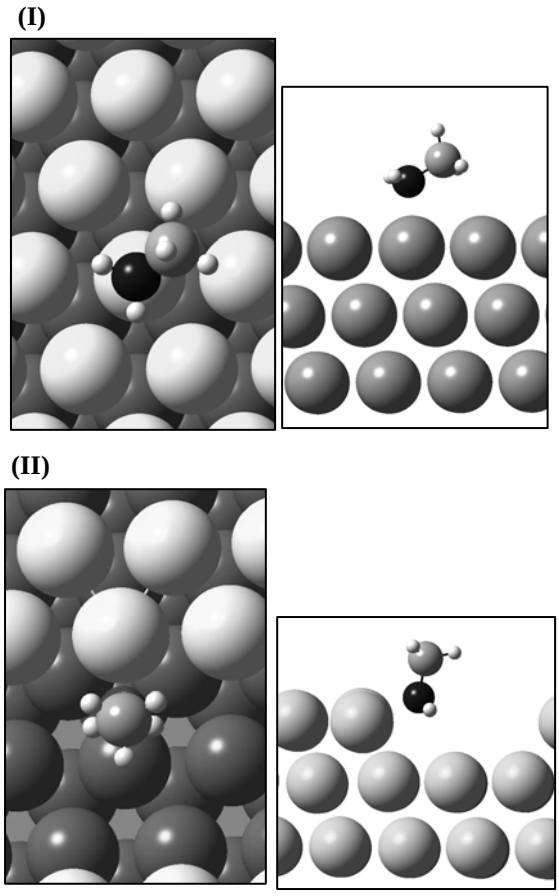

Fig. 3. Plan and side views of the gold surfaces showing the geometrical orientation of methylamine; bottom layers are darkened for clarity. (I) Adsorption on the Au(111) surface. (II) Adsorption on {111}/{111} ridge. Note: binding geometry on (100) and {111}/{100} ridge are similar to those on (111) and {111}/{111} ridge respectively, and are not presented here.

In a $2x10^{-4}$M solution of alkyl amine at room temperature (used in ref. 11), we estimated the fraction of bound sites on the (111), (100), {111}/{111} and {111}/{100} surfaces to be 0.1, 0.6, 0.99 and 0.99 respectively. With increasing particle size, the fraction of surface atoms located on the ridges will decrease, which reduces the overall surface coverage of the amine on the particle. This, we expect, will reduce the phase transfer efficiency of AuNS (from aqueous to organic phase) using alkyl amine as capping agent.

As discussed above, simple amines bind to AuNS

preferentially along the ridges over the flat surfaces by a factor of over 900. Linear molecules with multiple amine groups, such as ssDNA, could bind to a single AuNS at multiple sites. The connectivity of the amines through the backbone can greatly restrain the *local* geometry of the Au-amine at each bind site, causing a reduction in bond strengths. Hence in addition to binding strengths (as determined with simple methylamine), the preferred bind sites for these long-chain molecules will also depend on their tenacity to maintain strong binding even when the Au-amine geometry deviates from optimal. To further understand the roles played by different nanoparticulate surfaces on the adsorption of these multi-binding molecules, we examined how deviation from optimized Au-methylamine geometry can affect its binding strengths on these surfaces. Starting with the optimized geometry obtained in our earlier computations and keeping the position of nitrogen atom fixed, we performed geometrical transformations of the methylamine molecule and then computed binding energies for these under-optimized adsorbates. Rotation of the methylamine along the Au-N bond axis was found to have negligible effects (<0.05 kcal/mol) on binding strengths for all four surfaces. Fig. 4 illustrates these geometrical transformations on Au(111) surface and {111}/{111} ridge. This barrier-free rotation along the Au-N bond is characteristic of a single Au-N covalent bond, and it increases the versatility that long-chain molecules can bind at multiple sites. Next, we examined the effects of Au-N-C angle on binding energy. Fig. 5 shows how the binding energies decrease as the Au-N-C angles diverge from their optimal values. The response of binding energy to changes in Au-N-C angle is similar on the four surfaces. Importantly, binding on the ridges is invariably stronger than on the flat surfaces. The above analyses conclude that the ridges continue to be the preferred bind sites even when geometrical restrains do not permit optimal orientation of the amine around the Au atom, e.g. the case for ssDNA.

Since the ridges provide strong bind sites for amines, and assuming that ssDNA interact with gold via its amino groups, ssDNA-AuNS interaction is expected to increase with the fraction of the surface atoms located on the ridges. This fraction increases as the particle becomes smaller, as illustrated in Fig. 6. Indeed, attempts to assemble AuNS smaller than 5nm using thiol-modified DNA linkers were unsuccessful, which the authors attributed to strong interaction between DNA backbone and surface of these small AuNS [24]. This phenomenon may now be explained in the light of our results. On smaller particles the ridges are closely spaced, thereby allow ing ssDNA to bind onto a large multitude of ridge sites and favoring a collapsed form of the ssDNA on the particle. On the other hand, the ridges on larger particles are spaced further apart by weakly

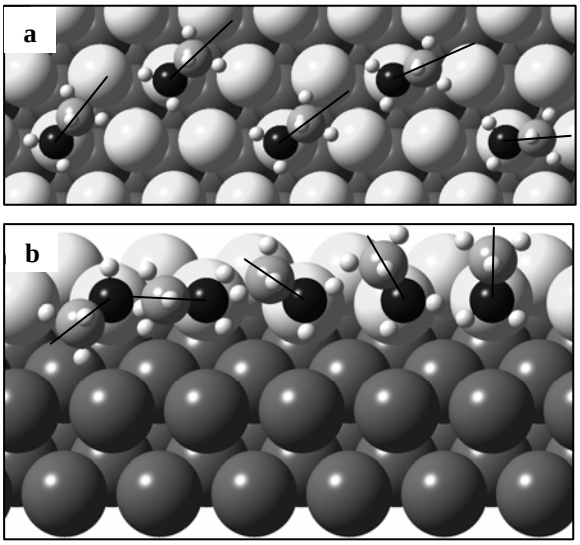

Fig. 4. Rotation of the methylamine molecule along the Au-N bond axis was found to have very little effect on its binding energy. Illustrated here are the geometries studied on **a.** Au(111) surface and **b.** {111}/{111} ridge. For clarity, the bottom Au layers are darkened, and guide-lines indicate N-C bond directions..

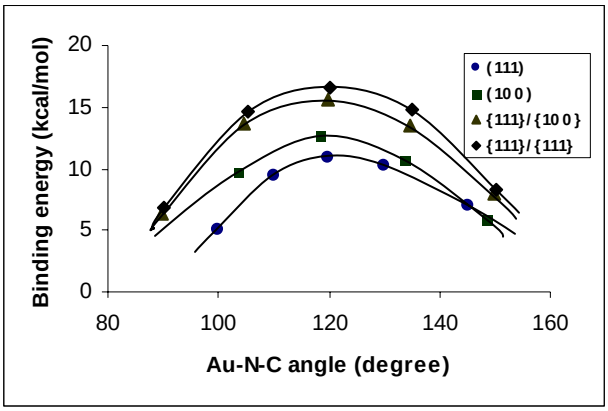

Fig. 5. Binding energy of methylamine on the four surfaces as the Au-N-C angles deviates from their optimal values. Invariably, the amine binds stronger on the ridges than on the flat surfaces

binding flat surfaces which limits the number of ridge sites that each ssDNA can makes contact with; in other words, a large fraction of the amines on the ssDNA "dangles" over the flat surfaces and have no access to the more reactive ridges. It is noteworthy that the hydrogen bond strength between double stranded DNA is about 5.5 kcal/mol. This is stronger than the binding on the flat surfaces, but weaker than that on the ridges. In effect, hybridization becomes increasingly hindered on smaller particles where binding at the ridges is more substantial. Particle size is hence an important controlling parameter to ensure DNA hybridization can take place on these nanoparticulate surfaces. It would be

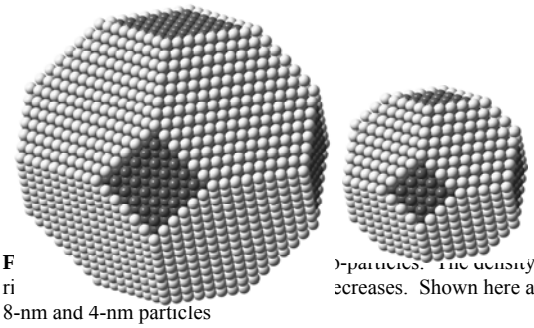

F)-particles. The density of ri ecreases. Shown here are 8-nm and 4-nm particles

of great interest to use computational methods to determine the smallest nanoparticle that has negligible effects on DNA hybridization. This would have to account for the complex dynamic interactions of random coil DNA with the gold surface, and may be achieved by carefully designed, albeit complex, molecular dynamic modeling. Such an analysis is beyond the current scope of work.

I. Conclusion

In conclusion, our DFT calculations show that methylamine binds to Au surfaces via interaction with a single Au atom. On AuNS, binding is enhanced substantially on the ridges than on the flat surfaces, which we propose explains the high reactivity of these nano-size particles towards amines. Also, our investigation on the effects of non-optimized Au-N-C geometry shows that the ridges are invariably the stronger bind sites even when the adsorbate is geometrically constrained. Based on the structural differences of the deoxynucleosides in DNA and experimental results of other workers, we propose that the interactions between ssDNA and AuNS may be attributed to the amine side groups of the deoxynucleotides and the ridges of the particles. This interaction is expected to increase as the particle size decreases and explains the inability to assemble small AuNS (<5 nm) using DNA linker; particle size is an important controlling parameter to ensure DNA hybridization is not hindered on these nanoparticulate surfaces. A better understanding of this interaction will facilitate the design of better AuNS-DNA conjugates for various applications, such as DNA detection.

References

[1] Fritzsche, W.; Taton, T. A., "Metal Nanoparticales as Lables for Heterogeneous, Chip-based DNA Detection (topical review)", *Nanotechnology* **2003,** 14, R63-R73.

[2] Nath, N.; Chilkoti, A., "Lable Free Colorimetric Biosensing Using Nanoparticles", *J. Fluoresc.* **2004,** 14, (4), 377-389

[3] Dubertret, B.; Calame, M.; Libchaber, A. J., "Single-mismatch Detection Using Gold-quenched Fluorescent Oligonucleotides", *Nat. Biotechnol.* **2001,** 19, 365-370K.

[4] Gueroui, Z.; Libchaber, A., "Single-Molecule Measurements of Gold-Quenched Quantum Dots", *Phy. Rev. Letts.* **2004,** 93, (16), 166108-1.

[5] Chang, E.; Miller, J. S.; Sun, J.; Yu, W. W.; Colvin, V. L.; Drezek, R.; West, J. L., "Protease-activated quantum dot probes", *Biochem. Biophy. Res. Co.* **2005,** 334, 1317-1321.

[6] Dyadyusha, L.; Yin, H.; Jaiswal, S.; Brown, T.; Baumberg, J. J.; Booy, F. P.; Melvin, T., "Quenching of CdSe quantum dot emission, a new approach for biosensing", *Chem. Commun.* **2005**, 3201

[7] Wargnier, R.; Baranov, A. V.; Maslov, V. G.; Stsiapura, V.; Artemyev, M.; Pluot, M.; Sukhanova, A.; Nabiev, I., "Energy transfer in aqueous solutions of oppositely charged CdSe/ZnS core/shell quantum dots and in quantum dot-nanogold assemblies", *Nano. Letters* **2004,** 4, (3), 451-457

[8] Nikoobakht, B.; Burda, C.; Braun, M.; Hun, M.; El-Sayed, M. A., "The quenching of CdSe quantum dots photoluminescence by gold nanoparticles in solution", *Photochem. Photobio.* **2002,** 75, (6), 591-597

[9] Oh, E.; Hong, M.-Y.; Lee, D.; Nam, S.-H.; Yoon, H. C.; Kim, H.-S., "Inhibition assay of biomolecules based on FRET between quantum dots and gold nanoparticles" *J. Am. Chem. Soc.* **2005,** 127, 3270-3271.

[10] Herne, T. M.; Tarlov, M. J., "Characterization of DNA Probes Immobilized on Gold Surfaces" *J. Am. Chem. Soc.* **1997,** 119, 8916-8920.

[11] Storhoff, J. J.; Elghanian, R.; Mirkin, C. A.; Letsinger, R. L., "Sequence-Dependent Stability of DNA-Modified Gold Nanoparticles" *Langmuir* **2002,** 18, 6666-6670.

[12] Jang, N. H., The Coordination Chemistry of DNA Nucleosides on Gold Nanoparticles as a Probe by SERS. *B. Kor. Chem. Soc.* **2002,** 23, (12), 1790-1800

[13] Sastry, M.; Kumar, A.; Mukherjee, P., "Phase Transfer of Aqueous Colloidal Gold Particles into Organic Solutions Containing Fatty Amine Molecules" *Colloids and Surfaces A* **2001,** 181, 255-259.

[14] Kumar, A.; Mandal, S.; Selvakannan, P. R.; Pasricha, R.; Mandale, A. B.; Sastry, M., "Investigation into the Interaction between Surface-Bound Alkylamines and Gold Nanoparticles" *Langmuir* **2003,** 19, 6277-6282.

[15] Xu, C.; Sun, L.; Kepley, L. J.; Crooks, R. M., "Molecular Interactions between Organized, Surface-Confined Monolayers and Vapor-Phase Probe Molecules. 6. In-situ FTIR External Reflectance Spectroscopy of Monolayer Adsorption and Reaction Chemistry" *Anal. Chem.* **1993,** 65, 2102-2107.

[16] Leff, D. V.; Brandt, L.; Heath, J. R., "Synthesis and Characterization of Hydrophobic, Organically-Soluble Gold Nanocrystals Functionalized with Primary Amines" *Langmuir* **1996,** 12, 4723-4730.

[17] Felice, R. D.; Selloni, A., "Adsorption modes of cysteine on Au(111): Thiolate, amino-thiolate, disulfide". *J. Chem. Phy.* **2004,** 120, (10), 4906-4914

[18] Whetten, R. L.; Khoury, J. T.; Alvarez, M. M.; Murthy, S.; Vezmar, I.; Wang, Z. L.; Stephens, P. W.; Cleveland, C. L.; Luedtke, W. D.; Landman, U., "Nanocrystal gold molecules" *Adv. Mat.* **1996,** 8, (5), 428-&.

[19] Landman, U.; Luedtke, W. D., "Small is different: energetic, structural, thermal, and mechanical properties of passivated nanocluster assemblies" *Faraday Discussions* **2004,** 125, 1-12.

[20] http://www.fysik.dtu.dk/campos/Dacapo/, DACAPO

[21] *Crystal data: determinative tables*. US Department of Commerce, National Bureau of Standards and Joint Committee in Powder Diffraction Standards: 1972; Vol. 2

[22] Khein, A.; Singh, D. J.; Umrigar, C. J., "All-electron Study of Gradient Corrections to the Local-Density Functional in Metallic Systems" *Phy. Rev. B* **1995,** 51, (7), 4105-4109

[23] Rizzo, R. C.; Jorgensen, W. l., "OPLS All-atom Model for Amines: Resolution of the Amine Hydration Problem" *J. Am. Chem. Soc.* **1999,** 121, 4827-4836

[24] Yang, J.; Lee, J. Y.; Too, H.-P.; Chow, G.-M.; Gan, L. M., "Triton X-100-Assisted Assembly of 5-nm Au Nanoparticles by DNA Hybridization" *Chem. Letts.* **2005,** 34, (3), 354-355